IEEE Access
Multidisciplinary | Rapid Review | Open Access Journal

Received December 7, 2018, accepted December 28, 2018, date of publication January 9, 2019, date of current version January 29, 2019.

Digital Object Identifier 10.1109/ACCESS.2019.2891988

A Multivariate Homogeneously Weighted Moving Average Control Chart

NURUDEEN A. ADEGOKE[1], SADDAM AKBER ABBASI[2], ADAM N. H. SMITH[1], MARTI J. ANDERSON[3], AND MATTHEW D. M. PAWLEY[1]

[1]School of Natural and Computational Sciences, Massey University, Albany, Auckland 0632, New Zealand
[2]Department of Mathematics, Statistics, and Physics, Qatar University, Doha 2713, Qatar
[3]New Zealand Institute for Advanced Study, Massey University, Albany, Auckland 0632, New Zealand

Corresponding author: Nurudeen A. Adegoke (nurudeen.adegoke@yahoo.com)

ABSTRACT This paper presents a multivariate homogeneously weighted moving average (MHWMA) control chart for monitoring a process mean vector. The MHWMA control chart statistic gives a specific weight to the current observation, and the remaining weight is evenly distributed among the previous observations. We present the design procedure and compare the average run length (ARL) performance of the proposed chart with multivariate Chi-square, multivariate EWMA, and multivariate cumulative sum control charts. The ARL comparison indicates superior performance of the MHWMA chart over its competitors, particularly for the detection of small shifts in the process mean vector. Examples are also provided to show the application of the proposed chart.

INDEX TERMS Average run length, control chart, manufacturing process, quality control, statistical process control.

I. INTRODUCTION

Rapid developments in data-acquisition in industry have led to increased interest in the joint monitoring of several related process parameters [1]. As a result, multivariate process control (MPC) methodology, in which several related process parameters are jointly monitored [2], is one of the most rapidly developing areas in statistical process control (SPC). Several MPC tools that use the relationships among the variables to provide efficient monitoring schemes for identifying any changes in the quality of the products have been proposed. These tools are capable of giving information as to when the process is in-control, provide diagnostic procedures for out-of-control situations, and are able to provide guidance on the overall process when it is out-of-control [3]. They are currently used in a range of scientific and technological application domains, including health-related monitoring, quality improvements, ecological monitoring, spatiotemporal surveillance, and profile monitoring [4].

MPC tools are generally applied in two monitoring phases [4]. In Phase I, a historical reference sample is analyzed to establish the values and stability of process parameters while in the in-control state. If the in-control parameter values are unknown, the data from Phase I are used to estimate these values and their control limits [5]. In Phase II, the process parameters are monitored and checked for departure from the in-control state. If Phase II values (or statistics) remain inside the in-control Phase I limits, the process is believed to be in control; if they go outside the control limits, this indicates that the process may be out-of-control and remedial actions are triggered.

Hotelling [6] was the first to propose and employ a multivariate process control tool; his χ^2 statistic represented the weighted Mahalanobis distance of the sample point from the center of the cloud and is known as the multivariate χ^2 control chart. This chart signals whenever the χ^2 values obtained from the process variable are greater than the chart's control limit $h = \chi^2_{p,\alpha}$ (where $\chi^2_{p,\alpha}$ is the α^{th} upper percentage point of the chi-square distribution and p is the number of quality characteristics being monitored). The multivariate χ^2 chart is a memoryless-type chart that uses only the most current process information and disregards any previous observations, and very efficient in detecting large shifts in the process mean vector.

To increase the sensitivity of the multivariate process control tool for the detection of small-to-moderate shifts in the process mean vector, different multivariate memory-type tools that use information from both the current and previous process observations have been proposed. For example, Crosier [7] and Pignatiello and Runger [8] proposed different possible multivariate extensions of the univariate cumulative sum (CUSUM) chart proposed by [9]. The multivariate exponentially weighted moving average (EMWA) control chart proposed by [10] is a multivariate extension of the univariate EWMA chart proposed by [11]. The memory-type charts are particularly effective for individual-observation monitoring [4].

In this article, we propose a new memory-type multivariate charting procedure, namely, the multivariate homogeneously weighted moving average (MHWMA) control chart. Like other memory-type charts, MHWMA uses the current observation and past observations. However, previous methods allocate equal weight across the observations, including the current one. With our proposed MHWMA method, the weight of the current observation can be specified, with the remaining weight then allocated equally across previous observations. We will show that this can provide more efficient monitoring of small shifts in the process mean vector, when compared to other memory-type multivariate charting procedures.

The remainder of this article is organized as follows. A review of the design structures of the multivariate exponentially weighted moving average (MEWMA) chart by [10], the multivariate cumulative sum #1 (MCI) chart by [8], and the multivariate cumulative sum (MCUSUM) chart by [7], respectively, are provided in Section II. The design of the MHWMA chart is discussed in Section III, and the run length performance of the chart is evaluated in Section IV. The ARL comparisons of the MHWMA chart with that of the χ^2 chart, MEWMA chart, MCUSUM chart, and MCI chart, respectively, are provided in Section V. Illustrative examples concerning the application of the proposed MHWMA chart are given in Section VI. Finally, conclusions and directions for future work are presented in Section VII.

In Appendix A, we derive the covariance matrix of the vector of HWMAs used with the MHWMA procedure. This matrix is used in Section III to obtain the MHWMA control-chart statistic. In Appendix B, we provide the proof of the dependency of the ARL performance of the MHWMA chart on the mean vector and covariance matrix only through the non-centrality parameter.

II. LITERATURE REVIEW: THE MEMORY-TYPE CONTROL CHARTS

Suppose we have $p \times n$ independently and identically distributed multivariate normal random variables $\boldsymbol{Y_1}, \boldsymbol{Y_2}, \ldots$, with mean vector $\boldsymbol{\mu_0}$ and covariance matrix $\boldsymbol{\Sigma_0}$. For monitoring the mean vector ($\boldsymbol{\mu_0}$) of an individual-observation (i.e., $n = 1$), the design structures of the memory-type charts are briefly described below:

A. THE MCUSUM CHART

Crosier [7] proposed two multivariate CUSUM charts. The one with better ARL performance obtains the CUSUM vector directly from the multivariate observation, and the MCUSUM vectors for the observed vector $\boldsymbol{y}_i$ are given as:

$$C_i = [(\boldsymbol{S_{i-1}}\ \mathcal{C}\ \boldsymbol{y_i} - \boldsymbol{\mu_0})' \boldsymbol{\Sigma_0^{-1}} (\boldsymbol{S_{i-1}}\ \mathcal{C}\ \boldsymbol{y_i} - \boldsymbol{\mu_0})]^{\boldsymbol{1/2}} \quad (1)$$

where

$$\boldsymbol{S_i} = \boldsymbol{0} \quad \text{if } C_i \le k$$
$$\boldsymbol{S_i} = (\boldsymbol{S_{i-1}}\ \mathcal{C}\ \boldsymbol{y_i} - \boldsymbol{\mu_0})(1 - k/C_i) \quad \text{if } C_i > k$$

$\boldsymbol{S_0} = \boldsymbol{0}$ and $k > 0$. The MCUSUM control chart signals when $T_i^2 = [\boldsymbol{S_i'} \boldsymbol{\Sigma_0^{-1}} \boldsymbol{S_i}] > h$.

B. THE MCI CHART

Two directionally invariant multivariate CUSUM charts were proposed by [8]; the one with better *ARL* performance is the MCI chart. Here, the CUSUM vectors for the observed vector $\boldsymbol{y_i}$ are given as:

$$\boldsymbol{C_i} = \sum_{j=i-n_i+1}^{i} (\boldsymbol{y_j} - \boldsymbol{\mu_0})$$
$$T_i = \max\left\{\sqrt{\boldsymbol{C_i'} \boldsymbol{\Sigma_0^{-1}} \boldsymbol{C_i}} - kn_i, 0\right\} \quad (2)$$

and

$$n_i = \begin{cases} n_{i-1} + 1, & \text{if } T_{i-1} > 0 \\ 1, & \text{if otherwise} \end{cases}$$

where n_i ($i = 1, 2, \ldots$), is interpreted as the number of subgroups up to the most recent cumulative sum statistic. The MCI control chart signals when $T_i > h$, for positive values of $h > 0$ and $k > 0$. The parameters of the MCUSUM and MCI charts, k and h, are chosen to give the desired in-control ARL performance of the chart [7], [8].

C. THE MEWMA CHART

The MEMWA control chart, proposed by [10], is a multivariate extension of the EWMA chart. It is a memory-type method that accumulates information from previous observations. The MEWMA statistics for the observed vector $\boldsymbol{y_i}$ are given as:

$$\boldsymbol{P_i} = r\boldsymbol{y_i} + (1 - r)\boldsymbol{P_{i-1}} \quad (3)$$

The use of small values for the smoothing parameter increases the power of the control chart and, if $r = 1$, the chart is identical to the memoryless control chart based on Hotelling's T^2.

The MEWMA chart gives an out-of-control signal when:

$$T_i^2 = (\boldsymbol{P_i} - \boldsymbol{\mu}_0)' \boldsymbol{\Sigma_{Pi}}^{-1} (\boldsymbol{P_i} - \boldsymbol{\mu}_0) > h \quad (4)$$

where h and r are chosen to achieve a desired in-control performance measure (such as a desired value of in-control *ARL*), and $\boldsymbol{\Sigma_{P_i}}$ is the covariance matrix at time point i. Lowry *et al.* [10] provided two alternative forms of $\boldsymbol{\Sigma_{P_i}}$: the exact covariance matrix is given as:

$$\boldsymbol{\Sigma_{P_i}} = \frac{r[1 - (1 - r)^{2i}]}{2 - r} \boldsymbol{\Sigma}_0 \quad (5)$$

and the asymptotic covariance matrix is given as:

$$\boldsymbol{\Sigma_P} = \frac{r}{2 - r} \boldsymbol{\Sigma}_0 \quad (6)$$

The MEWMA, MCUSUM and MCI charts are directionally invariant charts; the *ARL* performance of the charts depend on $\boldsymbol{\mu_0}$ and $\boldsymbol{\Sigma_0}$, only through the non-centrality parameter given as:

$$\delta = \sqrt{(\boldsymbol{\mu_1} - \boldsymbol{\mu_0})' \boldsymbol{\Sigma_0^{-1}} (\boldsymbol{\mu_1} - \boldsymbol{\mu_0})} \tag{7}$$

where $\boldsymbol{\mu_1}$ is the mean vector for the out-of-control process.

Several enhancements of these memory-type control charts in detecting small-to-moderate shifts have been proposed in SPC and related literature. For example, Hawkins *et al.* [12] proposed a self-starting MEWMA control charting for monitoring the process mean vector. Also, a self-starting control chart for multivariate individual observations monitoring was proposed by [13]. Kramer and Schmid [14] proposed EWMA charts for multivariate time series observation monitoring. Ngai and Zhang [15] proposed a MCUSUM control chart based on projection pursuit. Part and Jun [16] investigated a MEWMA control chart via multiple testing. Qiu and Hawkins [17] proposed a nonparametric MCUSUM procedure for detecting shifts in all directions. Qiu and Hawkins [18] proposed a rank-based MCUSUM Procedure. A multivariate sign EWMA control chart was proposed by [19]. A cumulative sum control charts for monitoring the covariance matrix [20]. A MEWMA control chart that can handle a non-constant smoothing parameter of the chart was proposed by [21]. An adaptive multivariate CUSUM control chart for signaling a range of location shifts was proposed by [22]. The performance of multivariate memory-type control charts with estimated parameters are investigated by [23]–[27].

III. THE MULTIVARIATE HOMOGENEOUSLY WEIGHTED MOVING AVERAGE (MHWMA) CONTROL CHART

To increase the sensitivity of the memory-type charts given in Section II in monitoring small shifts in the process mean vector, we propose a MHWMA control chart. The MHWMA control chart statistic gives a specific weight to the current observation, and the remaining weight is evenly distributed among the previous observations. The monitoring statistic of the proposed MHWMA chart is defined as:

$$\boldsymbol{H_i} = \boldsymbol{W}\boldsymbol{y_i} + (\boldsymbol{I} - \boldsymbol{W})\bar{\boldsymbol{y}}_{i-1} \tag{8}$$

where, $i = 1, 2, \ldots, ,\bar{\boldsymbol{y}}_{i-1}$ represents the sample average of the previous information up to and including the $i-1$ observation, and $\bar{\boldsymbol{y}}_0 = \boldsymbol{\mu}_0$. $\boldsymbol{W}$ is a $p \times p$ diagonal square matrix with smoothing or sensitivity parameters $w_k, k = 1, 2, \ldots, p$, along the diagonal such that $0 < w_k \leq 1$. The matrix $\boldsymbol{I}$ is a diagonal matrix of $1's$. If the values of the smoothing parameter, which determine the weight of each prior observation, are equal across variables, then the MHWMA vector becomes:

$$\boldsymbol{H_i} = w\boldsymbol{y_i} + (1 - w)\boldsymbol{y}_{i-1}^{-} \tag{9}$$

The MHWMA chart gives an out-of-control signal when

$$T_i^2 = (\boldsymbol{H_i} - \boldsymbol{\mu}_0)' \boldsymbol{\Sigma_{Hi}}^{-1} (\boldsymbol{H_i} - \boldsymbol{\mu}_0) > h \tag{10}$$

Here, h and w are chosen to achieve a desired in-control ARL performance measure, and $\boldsymbol{\Sigma_{Hi}}$ is the covariance matrix at time point i. From Appendix A, we have

$$\boldsymbol{\Sigma}_{H_i} = \begin{cases} w^2\boldsymbol{\Sigma}_0 & \text{if } i = 1 \\ w^2\boldsymbol{\Sigma}_0 + (1 - w)^2 \dfrac{\boldsymbol{\Sigma}_0}{i - 1} & \text{if } i > 1 \end{cases} \tag{11}$$

The MHWMA chart is a directionally invariant chart. In Appendix B, we give a proof that shows the relationship between the ARL performance and the non-centrality parameter given in equation 7.

SPECIAL CASES

- If $w = 1$, the monitoring statistic in equation (9) becomes:

$$\boldsymbol{H_i} = \boldsymbol{y_i} \tag{12}$$

and, $\boldsymbol{\Sigma_{Hi}}$ in equation (11) becomes:

$$\boldsymbol{\Sigma_{Hi}} = \boldsymbol{\Sigma}_0 \tag{13}$$

In this case, the MHWMA chart is identical to the memoryless χ^2 control chart, and we recommend monitoring either the χ^2 chart or the MHWMA chart (with $w = 1$).

- If $p = 1$, the monitoring statistic in equation (9) becomes:

$$H_i = wy_i + (1 - w)\bar{y}_{i-1} \tag{14}$$

and, the variance of the monitoring statistic H_i in equation (14) becomes:

$$\sigma_{H_i} = \begin{cases} w^2\sigma_0^2 & \text{if } i = 1 \\ w^2\sigma_0^2 + (1 - w)^2 \dfrac{\sigma_0^2}{i - 1} & \text{if } i > 1 \end{cases} \tag{15}$$

where σ_0^2 is the variance of a normally distributed univariate random variable. In this case, we recommend monitoring the proposed chart by [28].

- When $n > 1$, the vector $\boldsymbol{y}$ in the plotting statistic for the MHWMA vector in equation (9) can be replaced by the average of the *ith* sample (i.e, $\bar{\boldsymbol{y}}$). Hence, the covariance structure of the MHWMA chart becomes

$$\boldsymbol{\Sigma}_{Hi} = \begin{cases} \dfrac{w^2}{n}\boldsymbol{\Sigma}_0 & \text{if } i = 1 \\ \dfrac{w^2}{n}\boldsymbol{\Sigma}_0 + (1 - w)^2 \dfrac{\boldsymbol{\Sigma}_0}{n(i - 1)} & \text{if } i > 1 \end{cases} \tag{16}$$

IV. PERFORMANCE EVALUATION

In this section, we evaluate the performance of the proposed MHWMA chart by using different run length characteristics such as the average run length and standard deviation of the run length (SDRL) distribution. ARL is the most commonly used performance measures for control chart procedures. The in-control ARL (denoted by ARL_0), is the average number of plotted samples until an out-of-control signal is detected by a control chart when the process is in control. The out-of-control ARL (denoted by ARL_1), is the average number of

TABLE 1. ARL values for MHWMA charts ($p = 2$).

	w											
	0.03		0.05		0.2		0.4		0.6		0.8	
δ	ARL	$SDRL$	ARL	$SDRL$	ARL	$SDRL$	ARL	$SDRL$	ARL	$SDRL$	ARL	$SDRL$
0	199.26	202.01	199.35	182.57	202.99	186.06	201.63	192.36	200.54	201.62	200.39	199.06
0.05	166.24	197.29	173.00	157.48	186.94	169.67	193.77	189.26	194.31	190.36	199.62	198.50
0.10	115.64	132.81	129.55	119.99	154.16	136.29	177.88	173.09	184.99	185.98	192.07	194.5
0.25	43.05	44.91	53.32	46.28	74.00	60.41	107.64	102.17	139.03	137.16	161.6	160.77
0.50	15.80	14.3	19.87	15.56	27.50	19.5	41.84	36.4	64.86	62.32	91.91	90.24
0.75	8.56	6.83	10.65	7.7	14.50	9.24	19.25	15.5	31.66	29.95	50.15	49.11
1.00	5.70	4.09	6.91	4.52	9.23	5.31	10.94	7.96	16.54	14.56	27.24	26.23
1.50	3.32	2.04	3.90	2.22	4.85	2.48	5.05	3.05	6.3	4.8	9.69	8.71
2.00	2.32	1.4	2.67	1.49	3.19	1.49	3.13	1.62	3.41	2.2	4.54	3.63
2.50	1.74	1.06	1.99	1.16	2.35	1.12	2.22	1.05	2.26	1.2	2.66	1.79
3.00	1.37	0.79	1.53	0.9	1.81	0.9	1.7	0.76	1.7	0.79	1.86	1.07
5.00	1.00	0.08	1.01	0.09	1.03	0.17	1.03	0.16	1.03	0.18	1.03	0.17
	h											
	5.40		6.79		10.19		10.56		10.61		10.62	

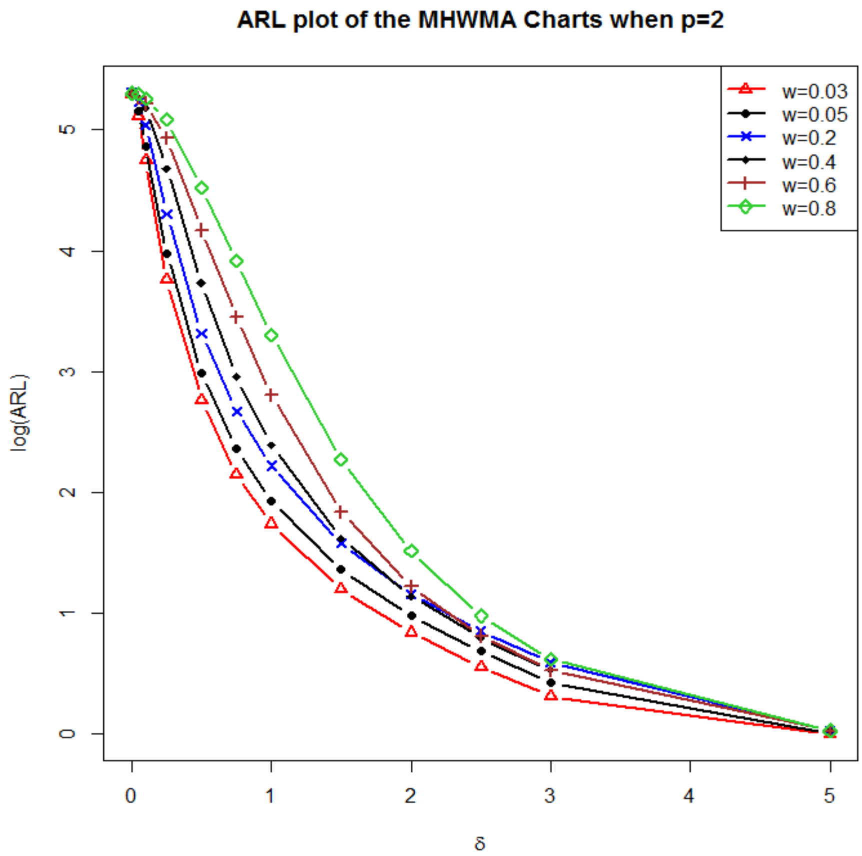

FIGURE 1. Plot of the logarithms of the ARL values given in Table 1.

plotted points until an out-of-control signal is detected by a control chart when the process is out of control [29]–[33]. It is generally desirable to have large values of ARL_0 and small values of ARL_1 for any control-chart setting [34]. The SDRL measures the spread of the run length distribution of the ARL [35]. Similarly, $SDRL_0$ and $SDRL_1$ can be defined.

The results are based on 10^5 Monte Carlo simulations, and δ denotes the shift size (given in equation (7)). The appropriate values of h are also obtained using simulation. The relative standard errors of the results in Table 1 and other findings in the paper are less than 1%. Table 1 reports the ARL and SDRL results for the case when $p = 2$ at varying levels of smoothing parameter (w) and shift (δ). The chart's parameters in Table 1 are chosen to fix the ARL_0 at 200. Visual representation of the logarithm of the ARL values in Table 1 are also provided in Figure 1. From the reported results in Table 1 (and/or Figure 1), we observe that:

TABLE 2. ARL values for MHWMA charts ($w = 0.1$).

	$p=2$				$p=3$				$p=4$			
						h						
δ	5.27	7.01	11.52	13.31	7.02	9.02	13.86	15.75	8.60	10.8	16.01	17.98
0	51.04	102.17	500.23	1000.53	51.01	103.07	502.15	997.44	50.07	102.32	498.68	1001.21
0.05	48.99	95.51	419.86	753.6	49.46	96.37	422.95	789.64	49.65	97.48	434.69	790.14
0.1	44.75	81.68	282.59	439.03	45.06	84.3	297.86	475.59	45.22	85.66	313.6	497.17
0.25	27.74	43.66	96.55	123.65	29.54	47.15	105.34	137.94	30.03	48.93	113.53	150.3
0.5	13.31	18.56	33.7	40.35	14.38	20.66	37.18	44.56	15.44	22.34	40.61	47.83
0.75	7.81	10.39	17.39	20.52	8.51	11.56	19.17	22.52	9.2	12.44	20.87	24.13
1	5.27	6.84	10.86	12.49	5.83	7.59	11.98	13.79	6.2	8.12	12.9	14.74
1.5	3.08	3.85	5.74	6.43	3.42	4.21	6.23	6.97	3.6	4.51	6.65	7.51
2	2.15	2.63	3.78	4.2	2.38	2.87	4.08	4.53	2.49	3.09	4.32	4.8
2.5	1.64	1.96	2.8	3.1	1.77	2.15	3.02	3.35	1.9	2.27	3.21	3.51
3	1.3	1.51	2.17	2.41	1.41	1.66	2.34	2.61	1.49	1.78	2.5	2.77
5	1	1.01	1.06	1.1	1.01	1.01	1.09	1.15	1.01	1.03	1.12	1.2

TABLE 3. SDRL values for MHWMA charts ($w = 0.1$).

	$p=2$				$p=3$				$p=4$			
						h						
δ	5.27	7.01	11.52	13.31	7.02	9.02	13.86	15.75	8.60	10.8	16.01	17.98
0	47.77	85.58	415.84	869.58	48.22	87.45	423.09	872.89	48.39	88.1	428.78	895.68
0.05	45.55	80.29	344.37	648.49	46.31	82.71	349.15	688.85	46.86	83.06	364.29	678.68
0.1	41.98	68.54	224.9	356.51	43.11	71.44	237.45	386.67	43.22	72.95	251.34	408.2
0.25	25.48	35.21	67.11	82.15	26.96	38.13	72.29	92.24	27.35	39.51	77.69	100.23
0.5	11.15	13.9	20.31	23.13	11.88	15	22.06	25.13	12.7	16.1	23.85	26.82
0.75	5.98	7.13	9.81	10.92	6.47	7.79	10.59	11.72	6.94	8.37	11.3	12.28
1	3.71	4.36	5.81	6.29	4.04	4.79	6.28	6.8	4.35	5.13	6.66	7.17
1.5	1.89	2.16	2.72	2.9	2.08	2.32	2.9	3.14	2.16	2.45	3.09	3.32
2	1.28	1.42	1.64	1.73	1.37	1.5	1.73	1.81	1.43	1.57	1.8	1.9
2.5	0.96	1.1	1.25	1.26	1.03	1.17	1.27	1.3	1.1	1.21	1.3	1.29
3	0.68	0.85	1.07	1.09	0.77	0.93	1.09	1.11	0.84	0.98	1.11	1.11
5	0.05	0.09	0.28	0.37	0.09	0.14	0.35	0.45	0.11	0.19	0.42	0.52

- Smaller values of w are more effective in detecting shifts in the mean vector. Specifically, the use of small values for the smoothing parameter increases the power of the MHWMA control chart.
- The proposed MHWMA chart is ARL unbiased, i.e., for any combinations of h and w, the ARL_1 values from the chart are always lesser than the ARL_0.
- The higher the ARL values of the chart, the higher the SDRL value as well.
- It is apparent that both ARL and SDRL decrease as the size of the shift increases. This indicates that larger shifts can be detected quickly and will result in a smaller spread in the run length distribution.

Tables 2-3 report the ARL and SDRL results for the case when $w = 0.1$ but with varying levels of p (i.e., $p = 2$, 3, and 4), and δ. The values shown for parameter h, in each case, are chosen such that the ARL_0 is fixed at 50, 100, 500, or $1,000$, respectively. We used $w = 0.10$, because small values of w are effective at detecting small shifts in the mean vector. From the reported results in Tables 2-3, we observe that:

- The ARL and SDRL performance of the chart depend on the number of quality characteristics (p). Specifically, the performance of the chart increases with the small value of p.
- The logarithm of the in-control ARL is very close to a linear function of the chart's upper limits. This property of the MHWMA chart can be used to approximate the appropriate value of the chart's control limits for other in-control $ARL's$.
- Larger shifts are detected quickly and result in a smaller spread in the run-length distribution.

V. AVERAGE RUN LENGTH COMPARISONS

In this section, the (zero-state) ARL performance of the MHWMA chart is compared with that of the χ^2 chart, the MCUSUM chart by [7], the MCI chart by [8], and the MEWMA chart by [10]. Since, the MEWMA, the MCUSUM, the MCI and the Hotelling's χ^2 charts are all directional invariant; these charts can be compared with each other and with the proposed MHWMA chart. We consider both the time-varying and the asymptotic limits MEWMA control chart.

The ARL values of the charts are presented in Tables 4 to 9, for $p = 2, 3, 4, 5, 10$ and 20, respectively. To allow reasonable comparisons of the proposed chart with the other charts, each chart is designed to give ARL_0 of approximately 200. We observed from Tables 4 to 9 that:

- The Hotelling's χ^2 chart, the MCUSUM chart, the MCI chart, and the MEWMA chart based on the asymptotic covariance structure (given in equation (6)), respectively, are all inferior to the proposed MHWMA chart (i.e., the MHWMA chart resulted in smallest values of the ARL_1) across all shifts.

TABLE 4. ARL comparisons for $p = 2$.

δ	χ^2; $h = 10.60$	MCI $k_1 = 0.50$, $h = 4.75$	MCUSUM; $k_2 = 0.5$, $h = 5.50$	MEWMA (5); $r = 0.1, 0$ $h = 8.79$	MEWMA (6); $r = 0.1$, $h = 8.66$	MHWMA; $w = 0.1$, $h = 8.965$
0.00	201.08	202.27	201.34	202.01	200.54	202.64
0.05	198.13	190.92	192.48	187.92	190.68	181.90
0.10	194.47	169.74	166.02	159.35	163.79	144.53
0.25	171.97	91.65	83.85	73.69	77.20	64.12
0.50	117.39	31.40	29.91	25.08	28.02	24.94
0.75	71.04	15.00	15.11	12.62	15.21	13.49
1.00	41.95	9.44	9.92	7.76	10.14	8.61
1.50	15.78	5.26	5.78	4.06	6.09	4.63
2.00	6.80	3.69	4.11	2.60	4.41	3.15
2.50	3.56	2.90	3.24	1.90	3.50	2.32
3.00	2.14	2.42	2.69	1.50	2.94	1.78
5.00	1.03	1.58	1.82	1.01	1.97	1.02

TABLE 5. ARL comparisons for $p = 3$.

δ	χ^2 $h = 12.85$	MCI $k_1 = 0.50$ $h = 5.48$	MCUSUM $k_2 = 0.5$ $h = 6.88$	MEWMA (5); $r = 0.10$ $h = 10.97$	MEWMA (6); $r = 0.1$ $h = 10.79$	MHWMA $w = 0.1$ $h = 11.09$
0.00	200.90	198.29	199.07	199.38	200.08	198.91
0.05	198.49	192.56	189.36	189.23	190.41	182.28
0.10	196.50	173.47	165.69	164.35	164.96	148.01
0.25	179.66	99.52	86.58	83.57	85.22	70.22
0.50	130.17	34.17	31.70	29.04	32.07	27.26
0.75	83.78	16.33	16.78	14.23	17.00	14.84
1.00	52.27	10.08	11.18	8.78	11.20	9.47
1.50	19.94	5.70	6.74	4.48	6.72	5.06
2.00	8.81	4.04	4.84	2.88	4.85	3.41
2.50	4.42	3.18	3.81	2.07	3.82	2.51
3.00	2.54	2.65	3.18	1.61	3.20	1.96
5.00	1.05	1.80	2.03	1.03	2.04	1.03

TABLE 6. ARL comparisons for $p = 4$.

δ	χ^2; $h = 14.86$	MCUSUM; $k_2 = 0.5$, $h = 8.15$	MEWMA; (5); $r = 0.10$, $h = 12.93$	MEWMA (6); $r = 0.1$, $h = 12.73$	MHWMA; $w = 0.1$, $h = 13.11$
0.00	199.67	198.82	200.35	201.31	202.48
0.05	199.22	189.39	192.01	192.38	185.14
0.10	196.49	166.35	170.33	170.00	157.64
0.25	182.25	86.83	90.02	94.14	74.38
0.50	139.90	33.24	31.94	35.25	30.01
0.75	94.32	18.28	15.54	18.40	16.32
1.00	61.12	12.46	9.45	12.05	10.21
1.50	24.27	7.57	4.83	7.23	5.42
2.00	10.77	5.47	3.07	5.17	3.62
2.50	5.16	4.33	2.21	4.09	2.71
3.00	2.93	3.61	1.71	3.41	2.09
5.00	1.07	2.20	1.04	2.11	1.05

- The simulation results show that the MHWMA chart detects shifts more rapidly than the MEMWA chart based on the exact covariance structure when $\delta \leq 0.5$. However, the ARL performance the MEWMA chart (given in equation (5)) is superior to the ARL performance of the proposed chart when there is a moderate-to-large shift in the mean vector. Specifically, the ARL_1 value of MEWMA chart based on the varying limit is smaller than the proposed chart when $\delta > 0.5$ is considered.

VI. ILLUSTRATIVE EXAMPLE

In this section, we provide a couple of examples for illustrating the application of the proposed MHWMA chart. The first example is based on a simulated dataset following [7], whereas, the second example is based on the bimetal dataset given in [36].

A. SIMULATED EXAMPLE

The dataset (see Table 10) is from a similar example given by [7], and also used for illustration in [10]. The data consists

TABLE 7. ARL comparisons for $p = 5$.

δ	χ^2; $h = 16.75$	MCI; $k_1 = 0.50$, $h = 6.81$	MCUSUM; $k_2 = 0.5$, $h = 9.46$	MEWMA (5); $r = 0.10$, $h = 14.74$	MEWMA (6); $r = 0.1$, $h = 14.56$	MHWMA; $w = 0.,1$ $h = 14.92$
0.00	201.27	204.29	200.10	201.17	201.09	201.25
0.05	199.91	194.57	191.99	192.94	193.66	187.90
0.10	198.00	178.31	175.26	172.87	174.92	159.04
0.25	184.88	109.22	91.95	95.63	99.13	77.97
0.50	143.82	38.74	35.81	34.40	38.35	31.38
0.75	102.37	17.72	19.95	16.71	19.83	17.08
1.00	68.25	11.04	13.71	10.12	12.91	10.78
1.50	28.44	6.39	8.47	5.16	7.65	5.79
2.00	12.27	4.60	6.16	3.24	5.47	3.85
2.50	6.00	3.64	4.87	2.34	4.31	2.82
3.00	3.35	3.03	4.05	1.80	3.60	2.23
5.00	1.10	2.01	2.53	1.06	2.20	1.08

TABLE 8. ARL comparisons for $p = 10$.

δ	χ^2; $h = 25.19$	MCUSUM; $k_2 = 0.5$, $h = 14.90$	MEWMA (5); $r = 0.10$, $h = 22.91$	MEWMA (6); $r = 0.1$, $h = 22.67$	MHWMA; $w = 0.1$, $h = 23.08$
0.00	200.03	198.63	195.71	204.11	199.09
0.05	199.15	192.01	194.58	197.11	190.02
0.10	198.4	170.55	173.78	182.80	162.23
0.25	190.45	96.34	114.45	117.35	89.52
0.50	162.01	42.89	45.20	47.94	37.53
0.75	124.50	25.96	21.47	24.94	20.86
1.00	92.80	18.62	12.60	15.85	13.05
1.50	44.70	11.92	6.38	9.19	6.87
2.00	20.60	8.80	3.97	6.57	4.52
2.50	9.90	7.02	2.78	5.15	3.36
3.00	5.20	5.86	2.13	4.28	2.64
5.00	1.24	3.63	1.12	2.69	1.19

TABLE 9. ARL comparisons for $p = 20$.

δ	χ^2; $h = 40.00$	MCUSUM; $k_2 = 0.5$, $h = 24.70$	MEWMA (5); $r = 0.10$, $h = 37.32$	MEWMA (6); $r = 0.1$, $h = 37.01$	MHWMA; $w = 0.1$, $h = 37.59$
0.00	202.01	199.21	198.61	200.78	202.12
0.05	199.98	193.02	194.59	197.51	193.61
0.10	198.73	175.36	185.65	187.59	173.59
0.25	193.11	109.37	130.76	135.51	102.77
0.50	173.05	55.99	58.31	63.09	46.24
0.75	145.62	36.65	27.89	32.27	25.60
1.00	116.96	27.18	16.32	20.16	16.34
1.50	66.53	17.94	7.99	11.28	8.50
2.00	34.46	13.50	4.90	8.00	5.47
2.50	17.26	10.81	3.40	6.26	4.01
3.00	9.07	9.05	2.59	5.20	3.13
5.00	1.58	5.57	1.29	3.19	1.44

of 10 observations, the mean is in-control at $\boldsymbol{\mu}_0 = (0, 0)$ for the first five observations and out-of-control at $\boldsymbol{\mu}_0 = (1, 2)$ for the last five observations. This example is illustrative of a moderate-to-large shift in the process mean vector, as the size of δ (in equation (7)) is approximately 2.65.

The first two columns of Table 10 give the sample of bivariate observations for the random variables Y_1 and Y_2. The columns H_1 and H_2 are the corresponding values of the MHWMA vector as provided in equation (9) using $w = 0.10$. The T^2 values obtained from equation (10) are given in the last column. For a fair comparison, the control limits were selected to give the desired ARL_0 of 200 for all the charts using $w = 0.10$. A plot of the MCUSUM chart with the same ARL_0 of 200, given by [7] (also reproduced in Figure 2), signals after the tenth observation. Plots of the MEWMA charts based on the exact and asymptotic limits of the same in-control ARL, given by [10], signals after the ninth and tenth observation, respectively. The plot of the MCI and MHWMA charts also signal an out-of-control situation after the tenth observation.

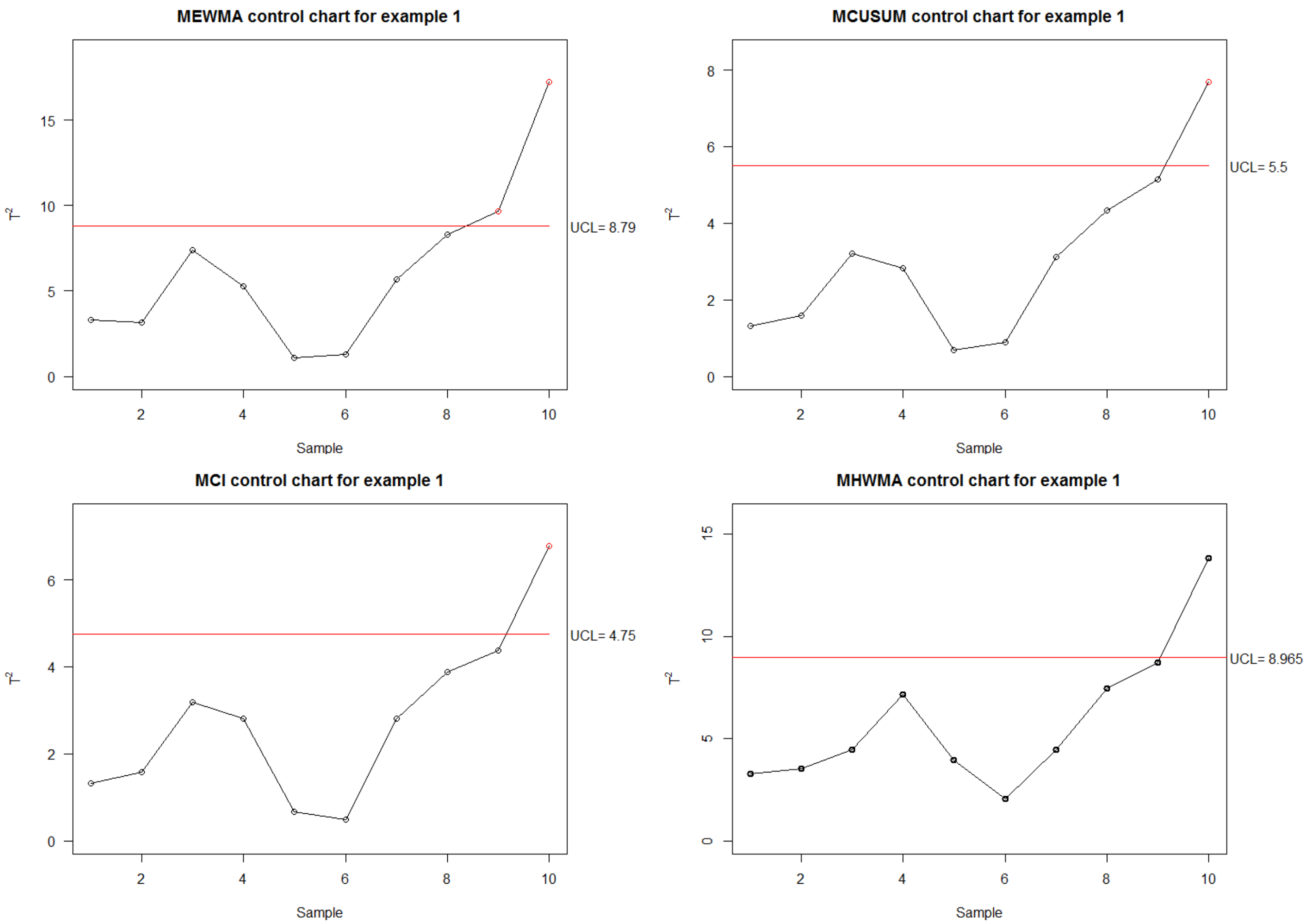

FIGURE 2. **Plots of the memory-type charts of the simulated dataset.**

TABLE 10. **The simulated dataset.**

	Observation		MHWMA vector		
n	Y_1	Y_2	H_1	H_2	T^2
1	-1.19	0.59	-0.12	0.06	3.29
2	0.12	0.9	-1.06	0.62	3.52
3	-1.69	0.4	-0.65	0.71	4.47
4	0.3	0.46	-0.80	0.61	7.15
5	0.89	-0.75	-0.46	0.45	3.97
6	0.82	0.98	-0.20	0.39	2.07
7	-0.3	2.28	-0.14	0.62	4.47
8	0.63	1.75	-0.07	0.80	7.45
9	1.56	1.58	0.11	0.90	8.71
10	1.46	3.05	0.26	1.12	13.85*
h					8.965

$*$ Out-of-control signal

B. BIMETAL THERMOSTAT DATASET EXAMPLE

For the second example, we used the bimetal thermostat dataset taken from [36]. The dataset contains measurements of the deflection, curvature, resistivity, and hardness for each of the low and high-expansion sides of brass and steel bimetal thermostats [37]. The process was employed in Phase I and Phase II, and data from the process at each phase consisted of sample size $m = 28$, and with $p = 5$ variables. The Phase I process is used to study a historical reference sample, which involves establishing the in-control state and evaluating the process stability to ensure that the reference sample is representative of the process. After this, the process parameters $\boldsymbol{\mu}_0$ and $\boldsymbol{\Sigma}_0$, are estimated from Phase I, and control chart limits are obtained to be used in Phase II. The Phase II aspect involves on-line monitoring of the process. In essence, any shift in the process needs to be detected quickly in Phase II, so that corrective actions can be taken at an early stage.

The estimated mean vector $(\hat{\boldsymbol{\mu}}_0)$ and covariance matrix $(\hat{\boldsymbol{\Sigma}}_0)$ are shown bottom of the next page.

Considering these estimates as the known parameters, we generated 20 Phase II observations from a multivariate normal distribution with mean $\boldsymbol{\mu}_1$ and covariance matrix $\hat{\boldsymbol{\Sigma}}_0$, such that the size of δ (in equation (7)) is approximately 0.087, which is a small shift in the mean vector. Specifically, we used, $\boldsymbol{\mu}_1 = (21.12, 40.12, 15.29, 22.12, 26.11)$. The inspiration for generating data in such manner is taken from [38] and [39]. The simulated bimetal Phase II data is given in Table 11.

The first five columns of Table 11 give the sample number (n) and the observations of the random variables: the

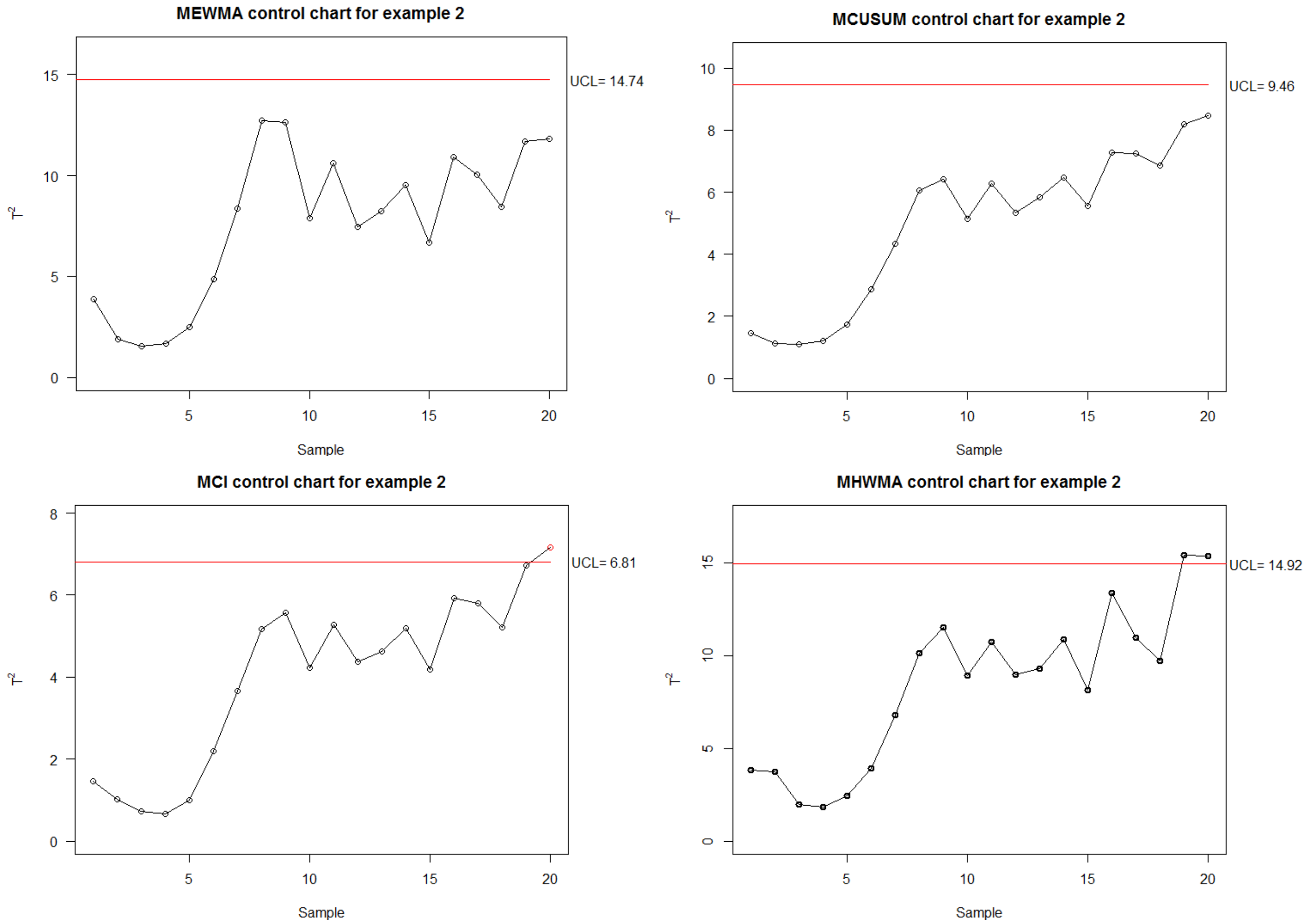

FIGURE 3. Plots of the memory-type charts of the bimetal dataset.

deflection (D), curvature (C), resistivity (R), Hardness low side (HL), and Hardness high side (HS). The columns H_1,H_2, H_3, H_4, and H_5 are the corresponding values of the MHWMA vector from equation (9) with $w = 0.10$. The T^2 values obtained from equation (10) are given in the last column. The values of the control limits and w were used to give an ARL_0 of 200. The control limits are obtained from Table 7 for all of the charts. The MEWMA chart with time-varying structure and the MCUSUM chart failed to detect the out-of-control signal (see Figure 3). The MCI chart detected the signal after the twentieth observation, while the MHWMA chart detected the shift in the mean vector after the nineteenth observation.

Although the MEWMA chart generally performed better than the other memory-type control charts to detect moderate-to-large shifts in the mean vector, the MHWMA chart was superior to the other methods when interest lies in detecting a small shift in the mean vector. Furthermore, the HWMA vector elements (in Tables 10, and 11) give an indication of the direction that the mean has shifted. This indication of the direction of the shift is common among memory-type control chart.

$$\hat{\mu}_0 = (21.01607, 40.01607, 15.19214, 22.02393, 26.01214)$$

$$\hat{\Sigma}_0 = \begin{array}{c} \\ \end{array}\begin{matrix} D & C & R & HL & HH \end{matrix}$$

$$\hat{\Sigma}_0 = \begin{pmatrix} 0.091877 & 0.025443 & 0.037909 & 0.027931 & 0.026753 \\ 0.025443 & 0.018543 & 0.026342 & 0.016131 & 0.016998 \\ 0.037909 & 0.026342 & 0.106284 & 0.016439 & 0.023377 \\ 0.027931 & 0.016131 & 0.016439 & 0.05444 & 0.011088 \\ 0.026753 & 0.016998 & 0.023377 & 0.011088 & 0.021477 \end{pmatrix} \begin{matrix} D \\ C \\ R \\ HL \\ HH \end{matrix}$$

TABLE 11. Simulated bimetal Phase II dataset.

	Observation					MHWMA vector					
n	D	C	R	HL	HH	H_1	H_2	H_3	H_4	H_5	T^2
1	21.37514	40.25279	15.36849	22.22992	26.28214	21.05198	40.03974	15.20978	22.04453	26.03914	3.848
2	20.74688	39.9778	14.95244	21.97061	25.94238	21.31232	40.22529	15.32689	22.20399	26.24817	3.727
3	21.47224	40.06028	15.344	22.18321	26.0622	21.10213	40.10979	15.17882	22.10856	26.10726	1.998
4	20.91048	40.10609	15.19133	21.95731	26.01251	21.16933	40.09787	15.21861	22.11085	26.08727	1.832
5	21.5028	40.04228	15.14889	22.16699	26.09236	21.16385	40.09355	15.20755	22.09343	26.07656	2.429
6	21.40367	40.23477	15.4103	22.36709	26.26783	21.22173	40.10254	15.22196	22.12816	26.09727	3.909
7	21.53276	40.23035	15.32421	22.16859	26.27788	21.26496	40.12414	15.24474	22.14813	26.1267	6.781
8	21.14701	40.1041	14.79022	21.71361	26.26096	21.26464	40.12669	15.20269	22.10555	26.14661	10.135
9	21.44861	40.16828	15.59713	22.16583	26.17052	21.2801	40.13028	15.23182	22.10178	26.15186	11.516
10	20.32414	39.9469	14.69693	22.21045	25.84648	21.18637	40.11237	15.18239	22.11336	26.12153	8.933
11	21.47476	40.33704	16.09065	22.44353	26.34193	21.21521	40.13483	15.27322	22.14638	26.14357	10.719
12	21.22772	40.02005	15.25308	22.12308	25.89487	21.2141	40.12152	15.26377	22.14135	26.11689	8.983
13	20.99839	40.07298	15.38705	22.26694	26.12767	21.19231	40.11835	15.27628	22.15421	26.12167	9.271
14	21.24963	40.15326	15.23967	22.36554	26.06599	21.20251	40.12289	15.27006	22.17274	26.11597	10.869
15	21.12245	39.97848	15.3732	21.93203	25.95203	21.19316	40.10758	15.28124	22.14316	26.101	8.131
16	21.82112	40.15864	15.32999	22.24247	26.27943	21.25831	40.11699	15.28305	22.16013	26.12381	13.387
17	20.94721	40.07874	15.3307	22.26007	26.03262	21.2061	40.11161	15.28606	22.16704	26.10885	10.957
18	20.73335	40.06492	15.37731	22.12997	26.00501	21.16948	40.10829	15.29335	22.1595	26.10161	9.724
19	21.35438	40.34669	15.51139	22.18066	26.35229	21.20736	40.13406	15.31142	22.16293	26.13097	15.388
20	21.3523	40.17716	15.04093	21.97396	26.14652	21.21489	40.1283	15.2749	22.14319	26.12204	15.37

The interpretation of out-of-control signals from multivariate control charts can be quite difficult. For a univariate control chart, an out-of-control state can be easily detected and interpreted, since a univariate chart is associated with only a single variable. However, this is not the case for the multivariate charts. Because the charts involve a number of correlated variables, the identification and interpretation of any out-of-control signals are not straightforward and has been an interesting topic in SPC literature. We refer the interested reader to [1] for guidance and recommendation on interpreting out-of-control signals in multivariate control charts. In line with [10], we recommend monitoring the principal components if these are interpretable. Different researchers, including [3], [40], and [41], among others, have proposed various principal-component methods to aid interpretation of out-of-control signals. For example, an MHWMA chart based on the first k principal components or the joint univariate control charts with standard or Bonferroni control limits across the p variables can be plotted.

VII. CONCLUSION AND DIRECTION FOR FUTURE WORK

In this paper, a new multivariate chart, namely, multivariate homogeneously weighted moving average (MHWMA) control chart, is proposed for the monitoring of process mean vector. The performance of the chart is evaluated and compared with multivariate χ^2, MEWMA, MCI and MCUSUM charts considering a variety of charting parameters. The run length comparison revealed that the proposed MHWMA chart is superior to the compared charts, particularly for the detection of small shifts in the process mean vector.

In future research, the inertia problem and robustness to non-normality of the proposed chart need to be investigated. Guidelines on the interpretation of out-of-control signals of the MHWMA chart also require further investigation. Also, the effect of parameter estimates on the Phase II performance of the chart needs to be investigated.

APPENDIX A
DERIVATION OF THE MEAN VECTOR AND COVARIANCE MATRIC OF H_i

From equation (9), we have that for an in-control situation: The mean vector of H_i is given as:

$$E(\boldsymbol{H_i}) = wE(\boldsymbol{Y_i}) + (1-w)E(\bar{\boldsymbol{Y}}_{i-1})$$
$$E(\boldsymbol{H_i}) = w(\boldsymbol{\mu}_0) + (1-w)(\boldsymbol{\mu}_0)$$
$$E(\boldsymbol{H_i}) = \boldsymbol{\mu}_0.$$

The covariance matrix of H_i is given as: when $i = 1$, we have

$$\boldsymbol{H_1} = w\boldsymbol{y_1} + (1-w)\boldsymbol{\mu_0}$$
$$Var(\boldsymbol{H_i}) = w^2\boldsymbol{\Sigma}_0 + (1-w)^2\, Var(\boldsymbol{\mu_0})$$
$$Var(\boldsymbol{H_i}) = w^2\boldsymbol{\Sigma}_0$$

when $i > 1$, we have:

$$Var(\boldsymbol{H_i}) = w^2\, Var(\boldsymbol{Y_i}) + (1-w)^2\, Var(\bar{\boldsymbol{Y}}_{i-1}) + 2w(1-w)Cov(\boldsymbol{Y_i}, \bar{\boldsymbol{Y}}_{i-1})$$

where, we have assumed that Y_i are independent and identical distributed. Hence, $Cov(\boldsymbol{Y_i}, \bar{\boldsymbol{Y}}_{i-1}) = 0$ for all pair of i and $i-1$.

$$Var(\boldsymbol{H_i}) = w^2\boldsymbol{\Sigma}_0 + (1-w)^2\frac{\boldsymbol{\Sigma}_0}{(i-1)},$$

Hence, the covariance matrix of H_i is given as:

$$\Sigma^2_{H_i} = \begin{cases} w^2\boldsymbol{\Sigma}_0 & \text{if } i = 1 \\ w^2\boldsymbol{\Sigma}_0 + (1-w)^2\dfrac{\boldsymbol{\Sigma}_0}{(i-1)} & \text{if } i > 1 \end{cases} \quad (17)$$

APPENDIX B

This proof that the distribution of the MHWMA test statistic H_i depends only on the value non-centrality parameter is based on the proof in [7] and [10]. The basic idea is to show that the values of H_i are invariant to any full-rank transformation of the data. That is, if $\boldsymbol{M}$ is a $p \times p$ full rank matrix and $y^* = My$, then the MHWMA statistics $\boldsymbol{H}_i$, and also, the T^2 value, have the same value when calculated from y^* as when calculated from y. Hence, $\boldsymbol{H}^* = \boldsymbol{MH}$. Reference [7] have chosen an orthogonal matrix $\boldsymbol{M}$ that diagonalizes $\boldsymbol{\Sigma}_0$. From equation (9), when $i = 1$, we have

$$\boldsymbol{H_1^*} = \boldsymbol{M}(w\boldsymbol{y_1} + (1-w)\boldsymbol{\mu_0}) = \boldsymbol{MH_1}$$

Hence, it follows that

$$\boldsymbol{T_1^{*2}} = \boldsymbol{H_1^{*\prime}\Sigma_{H_1}^{-1}H_1^*}$$
$$\boldsymbol{T_1^{*2}} = \boldsymbol{H_1^{\prime}M^{\prime}(M^{\prime -1}\Sigma_{H_1}^{-1}M^{-1})MH_1}$$

where, $\boldsymbol{M^{\prime}M^{\prime -1}} = \boldsymbol{M^{-1}M} = \boldsymbol{I}$

$$\boldsymbol{T_1^{*2}} = \boldsymbol{H_1^{\prime}\Sigma_{H_1}^{-1}H_1} = \boldsymbol{T_1^2}$$

When $i > 1$, we have:

$$\boldsymbol{H_i^*} = \boldsymbol{M}(w\boldsymbol{y_i} + (1-w)\boldsymbol{y}_{i-1}^{-}) = \boldsymbol{MH_i}$$

Hence, it follows that

$$\boldsymbol{T_i^{*2}} = \boldsymbol{H_i^{*\prime}\Sigma_{H_i}^{-1}H_i^*},$$
$$\boldsymbol{T_i^{*2}} = \boldsymbol{H_i^{\prime}M^{\prime}(M^{\prime -1}\Sigma_{H_i}^{-1}M^{-1})MH_i}$$
$$\boldsymbol{T_i^{*2}} = \boldsymbol{H_i^{\prime}\Sigma_{H_i}^{-1}H_i} = \boldsymbol{T_i^2}$$

The results in [7] can now be applied.

REFERENCES

[1] S. Bersimis, S. Psarakis, and J. Panaretos, "Multivariate statistical process control charts: An overview," *Qual. Rel. Eng. Int.*, vol. 23, no. 5, pp. 517–543, 2007.
[2] A. Seif, M. B. Moghadam, A. Faraz, and C. Heuchenne, "Statistical merits and economic evaluation of T^2 control charts with the VSSC scheme," *Arabian J. Sci. Eng.*, vol. 36, no. 7, pp. 1461–1470, 2011.
[3] J. E. Jackson, *A User's Guide to Principal Components*. Hoboken, NJ, USA: Wiley, 1991.
[4] D. Montgomery, *Introduction to Statistical Quality Control*, 6th ed. Hoboken, NJ, USA: Wiley, 2009.
[5] S. A. Abbasi and N. A. Adegoke, "Multivariate coefficient of variation control charts in phase I of SPC," *Int. J. Adv. Manuf. Technol.*, vol. 99, nos. 5–8, pp. 1903–1916, 2018.
[6] H. Hotelling, "Multivariate quality control-illustrated by air testing of sample bombsights," in *Techniques of statistical analysis*, M. W. H. C. Eisenhart and W. A. Wallis, Eds. New York, NY, USA: McGraw-Hill, 1947, pp. 111–184.
[7] R. B. Crosier, "Multivariate generalizations of cumulative sum quality-control schemes," *Technometrics*, vol. 30, pp. 291–303, Aug. 1988.
[8] J. J. Pignatiello and G. C. Runger, "Comparisons of multivariate CUSUM charts," *J. Qual. Technol.*, vol. 22, no. 3, pp. 173–186, 1990.
[9] Page, E. S, "Cumulative sum charts," *Technometrics*, vol. 3, no. 1, pp. 1–9, 1961.
[10] C. A. Lowry, W. H. Woodall, C. W. Champ, and S. E. Rigdon, "A multivariate exponentially weighted moving average control chart," *Technometrics*, vol. 34, no. 1, pp. 46–53, 1992.
[11] S. W. Roberts, "Control chart tests based on geometric moving averages," *Technometrics*, vol. 1, no. 3, pp. 239–250, 1959.
[12] D. M. Hawkins and E. M. Maboudou-Tchao, "Self-starting multivariate exponentially weighted moving average control charting," *Technometrics*, vol. 49, no. 2, pp. 199–209, 2007.
[13] J. H. Sullivan and L. A. Jones, "A self-starting control chart for multivariate individual observations," *Technometrics*, vol. 44, no. 1, pp. 24–33, 2002.
[14] H. G. Kramer and L. Schmid, "EWMA charts for multivariate time series," *Sequential Anal.*, vol. 16, no. 2, pp. 131–154, 1997.
[15] H.-M. Ngai and J. Zhang, "Multivariate cumulative sum control charts based on projection pursuit," *Statistica Sinica*, vol. 11, no. 3, pp. 747–766, 2001.
[16] J. Park and C.-H. Jun, "A new multivariate EWMA control chart via multiple testing," *J. Process Control*, vol. 26, pp. 51–55, Feb. 2015.
[17] P. Qiu and D. Hawkins, "A nonparametric multivariate cumulative sum procedure for detecting shifts in all directions," *J. Roy. Stat. Soc. D, Statistician*, vol. 52, no. 2, pp. 151–164, 2003.
[18] P. Qiu and D. Hawkins, "A rank-based multivariate CUSUM procedure," *Technometrics*, vol. 43, no. 2, pp. 120–132, 2001.
[19] C. Z. Tsung and F. Tsung, "A multivariate sign EWMA control chart," *Technometrics*, vol. 53, no. 1, pp. 84–97, 2012.
[20] L. K. Chan and J. Zhang, "Cumulative sum control charts for the covariance matrix," *Statistica Sinica*, vol. 11, no. 3, pp. 767–790, 2001.
[21] L. Yumin, "An improvement for Mewma in multivariate process control," *Comput. Ind. Eng.*, vol. 31, no. 3, pp. 779–781, 1996.
[22] T. Wang and S. Huang, "An adaptive multivariate CUSUM control chart for signaling a range of location shifts," *Commun. Statist. Theory Methods*, vol. 45, no. 16, pp. 4673–4691, 2016.
[23] L. A. Jones, C. W. Champ, and S. E. Rigdon, "The performance of exponentially weighted moving average charts with estimated parameters," *Technometrics*, vol. 43, no. 2, pp. 156–167, 2001.
[24] M. A. Mahmouda and P. E. Maravelakisb, "The performance of the MEWMA control chart when parameters are estimated," *Commun. Statist. Simul. Comput.*, vol. 39, no. 9, pp. 1803–1817, 2010.
[25] A. A. Aly, M. A. Mahmoud, and R. Hamed, "The performance of the multivariate adaptive exponentially weighted moving average control chart with estimated parameters," *Qual. Rel. Eng. Int.*, vol. 32, no. 3, pp. 957–967, 2016.
[26] C. W. Champ and L. A. Jones-Farmer, "Properties of multivariate control charts with estimated parameters," *Sequential Anal.*, vol. 26, no. 2, pp. 153–169, 2007.
[27] M. A. Mahmoud and P. E. Maravelakis, "The performance of multivariate CUSUM control charts with estimated parameters," *J. Stat. Comput. Simul.*, vol. 83, no. 4, pp. 37–41, 2013.
[28] N. Abbas, "Homogeneously weighted moving average control chart with an application in substrate manufacturing process," *Comput. Ind. Eng.*, vol. 120, pp. 460–470, May 2018.
[29] M. S. Aldosari, M. Aslam, N. Khan, L. Ahmad, and C. H. Jun, "A new S^2Control chart using multiple dependent state repetitive sampling," *IEEE Access*, vol. 6, pp. 49224–49236, 2018.
[30] M. Aslam, "Statistical monitoring of process capability index having one sided specification under repetitive sampling using an exact distribution," *IEEE Access*, vol. 6, pp. 25270–25276, 2018.
[31] M. Aslam, R. Bhattacharya, and M. S. Aldosari, "Design of control chart in presence of hybrid censoring scheme," *IEEE Access*, vol. 6, pp. 14895–14907, 2018.
[32] S. A. Abbasi, A. Miller, and M. Riaz, "Nonparametric progressive mean control chart for monitoring process target," *Qual. Rel. Eng. Int.*, vol. 29, no. 7, pp. 1069–1080, 2013.
[33] N. A. Adegoke, M. Riaz, R. A. Sanusi, A. N. Smith, and M. D. Pawley, "EWMA-type scheme for monitoring location parameter using auxiliary information," *Comput. Ind. Eng.*, vol. 114, pp. 114–129, Dec. 2017.
[34] S. Ahmad, S. A. Abbasi, M. Riaz, and N. Abbas, "On efficient use of auxiliary information for control charting in SPC," *Comput., Ind. Eng.*, vol. 67, no. 1, pp. 173–184, 2014.
[35] S. W. Human, P. Kritzinger, and S. Chakraborti, "Robustness of the EWMA control chart for individual observations," *J. Appl. Statist.*, vol. 38, no. 10, pp. 2071–2087, 2011.
[36] E. Santos-Fernandez, *Multivariate Statistical Quality Control Using R*. New York, NY, USA: Springer, 2012.
[37] N. A. Adegoke, A. N. H. Smith, M. J. Anderson, S. A. Abbasi, and M. D. M. Pawley, "Shrinkage estimates of covariance matrices to improve the performance of multivariate cumulative sum control charts," *Comput. Ind. Eng.*, vol. 117, pp. 207–216, Feb. 2018.
[38] R. A. Sanusi, M. Riaz, N. A. Adegoke, and M. Xie, "An EWMA monitoring scheme with a single auxiliary variable for industrial processes," *Comput. Ind. Eng.*, vol. 114, pp. 1–10, Dec. 2017.
[39] R. Singh and N. S. Mangat, *Elements of Survey Sampling*. Dordrecht, The Netherlands: Springer, 2013.
[40] T. Kourti and J. F. Macgregor, "Multivariate SPC methods for process and product monitoring," *J. Qual. Technol.*, vol. 28, no. 4, pp. 409–428, 1996.
[41] P. E. Maravelakis, S. Bersimis, J. Panaretos, and S. Psarakis, "Identifying the out of control variable in a multivariate control chart," *Commun. Statist. Theory Methods*, vol. 31, no. 12, pp. 2391–2408, 2002.

NURUDEEN A. ADEGOKE is currently pursuing the Ph.D. degree in statistics with the School of Natural and Computational Sciences, Massey University at Albany, Auckland, New Zealand. His current research interests include statistical process control, reliability, regularization procedures, ecological monitoring, and sampling techniques.

SADDAM AKBER ABBASI is currently an Assistant Professor with the Department of Mathematics, Statistics and Physics, Qatar University, Doha, Qatar. His research interests include statistical process control, time series analysis, profile monitoring, and nonparametric statistics.

ADAM N. H. SMITH is currently a Senior Lecturer in statistics with the School of Natural and Computational Sciences, Massey University at Albany, Auckland, New Zealand. His main research interests include the areas of the applied Bayesian modeling, multivariate analysis, biodiversity, and fisheries and marine ecology.

MARTI J. ANDERSON is currently a Distinguished Professor with the New Zealand Institute for Advanced Study, Massey University at Albany, Auckland, New Zealand. Her core research interests include the areas of multivariate analysis, community ecology, biodiversity, ecological monitoring, experimental design, and resampling methods.

MATTHEW D. M. PAWLEY is currently a Senior Lecturer in statistics with the School of Natural and Computational Sciences, Massey University at Albany, Auckland, New Zealand. His research interests include high-dimensional data monitoring, statistical process control, data mining and analytics, and applied statistics, among others.